Veterinary and Comparative Oncology

WILEY

Veterinary and Comparative Oncology

ORIGINAL ARTICLE OPEN ACCESS

Classification and Prognostication of B-Cell and T-Cell Multicentric Lymphoma in Dogs Using Serum MicroRNAs

Latasha Ludwig[1,2] | Heather Treleaven[1] | Roger Moorehead[3] | Robert A. Foster[1] | R. Darren Wood[1] | R. Ayesha Ali[4] | Geoffrey A. Wood[1]

[1]Department of Pathobiology, University of Guelph, Guelph, Ontario, Canada | [2]Department of Population Medicine and Diagnostic Sciences, Cornell University, Ithaca, New York, United States | [3]Department of Biomedical Sciences, University of Guelph, Guelph, Ontario, Canada | [4]Department of Mathematics and Statistics, University of Guelph, Guelph, Ontario, Canada

Correspondence: Geoffrey A. Wood (gewood@uoguelph.ca)

Received: 26 December 2024 | **Revised:** 19 March 2025 | **Accepted:** 28 March 2025

Funding: This work was supported by Ontario Veterinary College, University of Guelph; OVC Pet Trust (Grant 55680); Natural Sciences and Engineering Research Council of Canada (Discovery and Vanier Canadian Graduate Scholarship) (Grant 401622).

Keywords: dog | lymphoma | microRNAs | serum

ABSTRACT

Canine multicentric lymphoma is a common malignancy in dogs. It often responds well to initial chemotherapy but frequently relapses and has a poor response to subsequent treatment. B-cell (BCL) and T-cell (TCL) lymphomas differ in both their prognoses and chemotherapeutic treatment protocols. Currently, immunophenotyping can be costly and can only be performed on specific high-quality samples. MicroRNAs (miRNAs) are small molecules present in blood and tissues and are dysregulated in both human and canine lymphoma. We investigated 59 miRNAs by RT-qPCR to establish a serum miRNA profile in dogs with B-cell and T-cell multicentric lymphoma. Multiple miRNA pruned decision tree models were used to classify BCL and TCL cases from each other and controls, and to predict prognosis in BCL cases receiving standard CHOP chemotherapy. Six individual miRNAs were differentially expressed in serum between BCL and controls, and three were differentially expressed between BCL and TCL. A three-miRNA model (miR-155-5p, miR-1 and miR-181b) could differentiate between BCL, TCL and control samples with an accuracy of 83.02%. A three-miRNA model (miR-125b-5p, miR-350 and let-7b-5p) in BCL samples separated the cases into four groups with hazard ratios ranging from 0.44 to 3.5 for overall survival. This study established a serum miRNA profile for both BCL and TCL and demonstrated the utility of multiple serum miRNA models to assist in the diagnosis of lymphoma and BCL prognostication.

1 | Introduction

Canine lymphoma is a common malignancy, with most cases being peripheral and multicentric [1–3]. After detection of an enlarged lymph node, fine needle aspiration and cytologic examination usually provide the diagnosis [4]. This is generally followed by grading, determination of clinical stage and immunophenotyping. Immunophenotyping requires flow cytometry, immunohistochemistry and/or PCR for antigen receptor rearrangement [5]. These are costly techniques which require advanced expertise and specific high-quality samples to provide reliable results [5]. Most cases of lymphoma are intermediate- to high-grade by histopathology and at an advanced stage of disease (III-IV) carrying a worse prognosis [1]. High-grade T-cell lymphomas (TCL) have a worse prognosis than high-grade B-cell lymphomas (BCL) [1]. However, even within these high-grade immunophenotypes, variation exists in prognosis [6, 7]. As such, novel biomarkers providing a cost-effective method of phenotyping and prognostication are required.

Standard-of-care treatment is multi-agent chemotherapy, with BCLs receiving CHOP protocols (cyclophosphamide [C], doxorubicin [H, hydroxydaunorubicin], vincristine [O, Oncovin] and prednisone [P]) and TCLs receiving more variable chemotherapeutic agents [1]. With these protocols, 80%–95% of patients will go into remission with a median survival time (MST) of 10–12 months, but most cases relapse, and reinduction/rescue protocols are often ineffective [1]. Detection of lymphoma at an earlier stage would allow a localised approach to treatment, such as surgery or radiation [1]. This would delay the use of chemotherapy and the subsequent development of chemoresistance.

MicroRNAs (miRNAs) are small non-coding RNA molecules that are present in the circulation, making them easily accessible [8, 9]. Along with their known stability in serum and plasma, this makes miRNAs an excellent candidate biomarker [9–12]. MiRNAs are dysregulated in both human and canine lymphoma; however, studies investigating their utility in the circulation are limited [4, 13–18]. Fujiwara-Igarashi et al. (2015) investigated a small number of serum samples from common lymphoma locations in which they found five miRNAs to be differentially expressed in cases of lymphoma compared with controls. MiR-25 could classify high- and low-grade cases [16]. Craig et al. (2019) investigated miRNAs in both plasma and lymph node aspirates and found numerous differentially expressed miRNAs and miRNAs that were prognostic in BCL and TCL cases [4].

Current literature supports multiple miRNA models as superior to single miRNAs in diagnosis and prognosis [19]. Behesti et al. (2019) found a five-miRNA signature in human serum samples with a classification rate of 91% between patients with diffuse large B-cell lymphoma (DLBCL) and controls [20]. These studies are lacking in canine lymphoma. As such, we investigated the miRNA profiles of serum samples from dogs with BCL or TCL and controls followed by multiple miRNA models for both diagnosis and prognosis of BCL.

2 | Materials and Methods

2.1 | Samples

Owner consent was obtained and an animal utilisation protocol (AUP 4409) was approved by the University of Guelph's Animal Care Committee. Serum samples were received from the Ontario Veterinary College's Veterinary Biobank. All cases involved the peripheral lymph nodes, and a diagnosis of lymphoma was confirmed by either cytology or histopathology with associated immunophenotyping (either flow cytometry or immunohistochemistry) into B- ($n = 24$) or T-cell ($n = 16$) subtypes. In all but one case, serum samples were taken at the time of first presentation to the Ontario Veterinary College Animal Cancer Centre for further assessment and/or initial treatment. Serum samples were obtained from control dogs ($n = 13$) with no history of malignancy at the time of collection. Eleven of the 13 control dogs had at least 1 year of clinical follow-up, one patient was lost to follow-up after 9 months and one patient was lost to follow-up after 1 month. Eleven of 13 normal dogs had a known cause of death unrelated to malignant neoplasia.

2.2 | Hemolysis Assessment

Each sample was assessed for hemolysis using the NanoDrop 2000 where UV-absorbance at 414 nm (A414) and 375 nm (A375) was measured (Supporting Information Materials S1). For each miRNA, the effect of hemolysis on its expression was assessed in two ways as previously described [21]. Briefly, a miRNA's Ct value from each sample was plotted against its A414, and a linear trendline was estimated, and an R^2 value was calculated (Supporting Information Materials S2) [22]. Additionally, samples were divided into hemolysed and non-hemolysed groups based on an A414 > 0.2 or A414/375 > 1.4, classifying samples into the hemolysed group [23, 24]. A Mann–Whitney *U* test was used to test for differences between these groups.

2.3 | Target miRNA Selection

Similar to Craig et al. and Ludwig et al., a pilot study of 5 pooled serum samples using the canine miScript miRNome miRNA arrays (QIAGEN) was performed [4, 21, 25]. Three groups of 5 BCL and control samples (two non-hemolysed and one hemolysed) and two groups of 5 TCL samples (one non-hemolysed and one hemolysed) were evaluated (Supporting Information Materials S3). As previously described by Ludwig et al., 200 μL of pooled sample was used per group for miRNA isolation [21, 25]. Briefly, each pooled sample's miRNA isolate was converted into complementary DNA (cDNA) with the miScript II RT Kit (QIAGEN) by reverse-transcription polymerase chain reaction (PCR) using the manufacturer's protocol. A master mix was created using the corresponding miScript SYBR green kit (QIAGEN) per the manufacturer's protocol. A Roche LC480 LightCycler was used for RT-qPCR set to QIAGEN's recommended settings. The LC480 software (release 1.5.1.62 SP3) calculated Ct values using the second derivative maximum method. A total of 59 miRNAs with the largest fold-changes between groups alongside miRNAs previously reported in the literature and additional controls were added to the custom miRCURY LNA PCR array design (QIAGEN) (Supporting Information Materials S4).

2.4 | Targeted Real-Time Quantitative Polymerase Chain Reaction

MiRNA isolation and RT-qPCR were performed as per Ludwig et al. [25] A standard volume of 200 μL from each serum sample was used to isolate small RNA species with the QIAGEN miRNeasy Serum/Plasma Advanced Kit following the manufacturer's protocol. Three and a half microliters of cel-miR-39-3p spike-in control was added (per the manufacturer's recommendations). At the final step, 15 μL RNase-free water was added to the centre of the spin column. Two microliters of the isolate was used to quantify the concentration with the Qubit microRNA Assay Kit and Qubit 2.0 Fluorometer (Invitrogen) (Supporting Information Materials S1).

A standard input of 0.6 μL of serum sample miRNA isolate was used for each reverse-transcription PCR to obtain 10 μL of cDNA following the manufacturer's protocol of the QIAGEN miRCURY LNA RT Kit. The C1000 Bio-Rad Thermo Cycler was used as previously described [25]. A no-template control (NTC) was included for each plate's samples, replacing the sample volume with water.

The cDNA from each sample was diluted to 1:40 before creating a master mix (miRCURY SYBR green kit (QIAGEN)) of SYBR green, diluted cDNA and nuclease-free water as per the manufacturer's protocol. For each miRCURY LNA miRNA custom PCR array (384-well; QIAGEN), a Roche LC480 LightCycler set to the SYBR Green I/HRM Dye detection format with a 10 μL volume reaction was used for RT-qPCR. Each PCR array was incubated as per the settings described by Ludwig et al. [25] The LC480 software (release 1.5.1.62 SP3) calculated *Ct* values using the second derivative maximum method.

2.5 | Quality Assessment of RT-qPCR Results

Each *Ct* value was subtracted by the difference between the average UniSp3 (IPC) of the NTC (up to 6 replicates per plate) for each PCR array and the overall average to get an IPC-corrected *Ct* value. The amplification and melting curves were manually assessed to ensure appropriate *Ct* determination by the LC480 software. All undetectable *Ct* values ($Ct = 0$), those > 35.00, and those with visually inappropriate amplification curves were changed to equal 35.00 to provide a conservative *Ct* determination. All further analyses used the IPC-corrected, conservative *Ct* values, from now on referred to as *Ct* values. All cel-miR-39-3p and UniSp6 values of samples included in the study were within the average of all samples ± two standard deviations. Samples and miRNAs must have had sufficient overall expression to be included in further analyses. Cutoffs were calculated as the average number of unexpressed miRNAs plus two standard deviations or non-expressing samples plus two standard deviations, for samples and miRNAs respectively, and those above these cutoffs were excluded. This included six miRNAs (hsa-miR-182-5p, hsa-miR-190b, hsa-miR-193b-5p, hsa-miR-206, cfa-miR-409 and cfa-miR-1844).

2.6 | Statistical Analysis

R Studio environment, software version 4.1.0. (R Core Team, 2021) was used for all statistical analyses [26]. The NormFinder R script was used to select stably expressed miRNAs as endogenous controls [27]. The controls, BCL and TCL samples, were assigned to groups for consideration in analysis. The miRNAs needed to be expressed in all samples ($Ct < 35.00$) and not associated with hemolysis to be considered a candidate endogenous control. At least 3 controls were selected: bta-miR-27a-3p, cfa-miR-23a and hsa-miR-502-3p, and *Ct* values averaged [21, 25, 28]. Normalisation was performed by the comparative *Ct* method, and the geometric average was used [21, 25, 28, 29].

Thirty percent of miRNAs were non-normally distributed by a Shapiro–Wilk test for normality, and so non-parametric tests were used. With normalised *Ct* values (ΔCt), the Wilcoxon rank-sum test was performed, and to correct for multiple testing, the Benjamini–Hochberg procedure was used [30]. A p value of < 0.05 was considered statistically significant. Fold changes were calculated using $2^{-\Delta\Delta Ct}$, where $\Delta\Delta Ct$ is the median ΔCt for a miRNA of interest in one group subtracted from the median ΔCt of the second group. Fold difference was equivalent to fold change when the value was ≥ 1, while fold difference was equivalent to the negative inverse of the fold change when the value was < 1.

A pruned decision tree model was used to assess the ability of multiple miRNAs to diagnose and accurately classify BCL and TCL samples and control samples. Decision trees were grown using the rpart() package with all miRNAs considered as variables. Pre-pruning was done to avoid overfitting by setting the minsplit parameter to 12 to restrict growth. A cost matrix was applied which designated false negatives as 3× more costly than a false positive. Receiver operating characteristic (ROC) curves were created using the pROC package. Accuracy, precision and recall metrics, along with a 95% confidence interval for the accuracy, were calculated for each class.

Each miRNA was assessed for prediction of overall survival (OS). OS was defined from the date of sample collection until the date of euthanasia. The date of sample collection generally corresponded to the date of initiation of chemotherapy. Patients whose cause of death was not related to lymphoma progression were censored. High and low expression groups for each miRNA based on survival data were determined using the surv_cutpoint() and surv_categorize() functions, in the survminer package in R by establishing the optimal cut-off ΔCt point [31]. The minprop value of 0.2 was used in surv_cutpoint() indicating a minimum proportion of 20% of samples must be allocated to either expression group. Kaplan–Meier curves were generated from each miRNA using ggsurvplot() and the log-rank test was used to calculate p values, where < 0.05 was considered statistically significant. A prognostic pruned decision tree model was developed for the BCL cases only. The OS decision tree was grown using rpart() and pre-pruned using a minsplit value of 10. Mean deviance was determined for each node's hazard ratio. Kaplan–Meier survival curves were used to assess differences in survival between the groups and statistical significance was determined using a log-rank test with survdiff() between each pairwise group comparison. The Bonferroni correction was applied to account for multiple comparisons and a p value < 0.05 was considered statistically significant.

3 | Results

Detailed demographic and clinical information are available in Supporting Information Materials S5–S7. Mixed breed was the most common in the BCL and control populations and Boxers in the TCL population. The median ages were 7.6, 6.9 and 9.0 years for the BCL, TCL and control groups, respectively. Castrated males were the most common in all groups. One TCL case was excluded from prognostic analyses due to incomplete medical records. In the BCL population, 21/24 cases were euthanised related to confirmed or suspected progressive disease and all patients received CHOP as their initial chemotherapeutic protocol. Seven cases did not complete

TABLE 1 | The miRNAs most (as per miR-16-5p, miR-92a-3p, miR-451a) and least (as per miR-21-5p) likely to be associated with hemolysis determined by the linear relationship between A414 and expression (R^2 value) and statistical significance between hemolysed and non-hemolysed groups (p value).

miRNA	R^2 value	p value of comparison
miRNAs likely associated with hemolysis		
miR-505-5p	0.48	9.30E-04
miR-16-5p	0.46	7.90E-04
miR-451a	0.38	5.10E-05
miR-25-3p	0.38	3.70E-04
miR-15a	0.36	3.80E-03
miR-15b	0.32	1.80E-04
miR-18a-5p	0.32	7.50E-03
miR-92a-3p	0.30	3.00E-02
miRNAs unlikely associated with hemolysis		
miR-21-5p	0.039	3.30E-01
miR-203a-3p	0.030	9.20E-01
miR-502-3p	0.022	3.20E-01
miR-1	0.009	9.50E-01
miR-155-5p	0.006	8.70E-01

their CHOP protocol due to adverse clinical signs and/or progressive disease. The MST was 377 days. Euthanasia was due to progressive disease in 12/15 of the TCL cases. Seven cases received CHOP alone as their initial chemotherapeutic treatment. The MST was 190 days.

MiR-16-5p, miR-92a-3p, miR-451a are known to be associated with erythrocytes and hemolysis and therefore served as a reference in this evaluation [21, 23, 25, 32, 33]. The R^2 value of the linear relationship for miR-16-5p, miR-92a-3p and miR-451a was 0.46, 0.30 and 0.38, respectively. Hemolysed and non-hemolysed groups were created using the parameters described above and compared. The p value for this comparison for miR-16-5p, miR-92a-3p and miR-451a was <0.05. Based on these results, any miRNA with an R^2 value greater than 0.30 and with a statistically significant p value between the group comparisons was considered likely associated with hemolysis (8 miRNAs; Table 1). The miR-21-5p is not associated with hemolysis in the literature [22, 32]. This miRNA had an R^2 value of 0.039 and a comparison p value of 0.33. Thus, any miRNAs with an R^2 value <0.039 and a non-significant p value were considered unlikely to be associated with hemolysis and included 5 miRNAs (Table 1). The relationship of other miRNAs is reported in Supporting Information Materials S8.

Three miRNAs had a significant increase in expression and three miRNAs had a significant decrease in expression in lymphoma samples compared with controls (Table 2 and Figure 1A). The miR-125a, miR-130b-3p, miR-145 and miR-155-5p had a median fold-difference $>\pm2$. Three miRNAs had significantly increased

TABLE 2 | Significantly ($p<0.05$) differentially expressed serum miRNAs in lymphoma (B-cell and T-cell) and control cases.

miRNA	Median fold-difference	p value (with Benjamini–Hochberg correction)
All lymphoma ($n=40$) vs. controls ($n=13$)		
miR-155-5p	2.73	1.81E-02
miR-130b-3p	2.10	3.60E-03
miR-574-3p	1.91	1.81E-02
miR-1	−1.94	1.90E-02
miR-125a	−2.05	3.60E-03
miR-145	−2.17	1.81E-02
B-cell lymphoma ($n=24$) vs. controls ($n=13$)		
miR-155-5p	4.34	4.33E-04
miR-150-5p	2.92	1.67E-02
miR-130b-3p	2.20	3.40E-03
miR-1	−2.05	2.55E-02
miR-125a	−2.47	4.33E-04
miR-145-5p	−3.00	9.51E-03
T-cell lymphoma ($n=16$) vs. B-cell lymphoma ($n=24$)		
miR-130a-3p	2.47	2.18E-02
miR-181a	1.95	2.81E-02
miR-155-5p	−3.51	1.30E-02

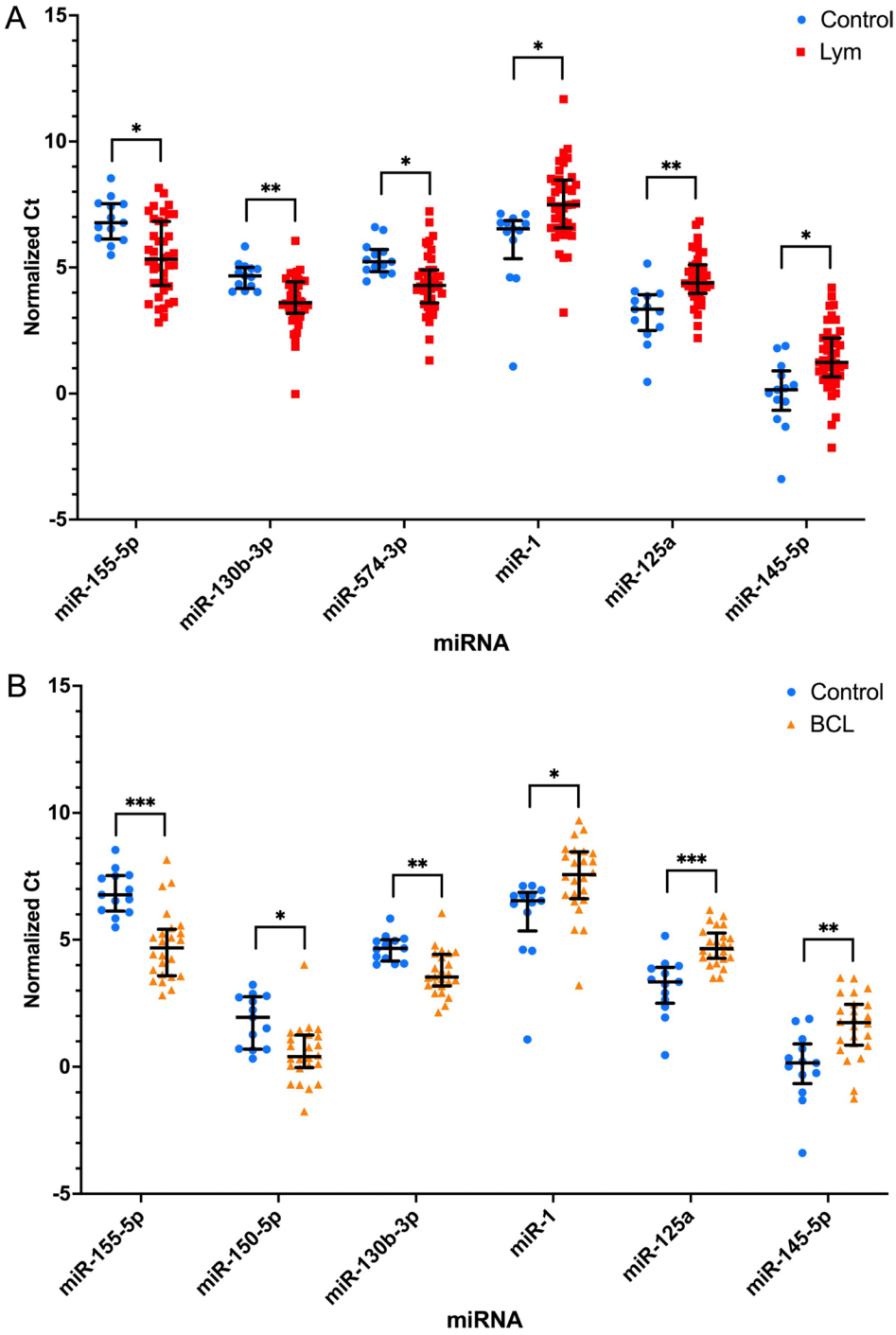

FIGURE 1 | The miRNAs significantly (p value <0.05) differentially expressed between lymphoma groups and controls. Values are shown as normalised cycle threshold (*Ct*) values. *p value <0.05, **p value <0.01, ***p value <0.001. Benjamini–Hochberg corrected p values. Bar represents median with interquartile range. (A) Differentially expressed miRNAs in all lymphoma (Lym) samples compared with controls. (B) Differentially expressed miRNAs in B-cell lymphoma (BCL) samples compared with controls.

expression and three miRNAs had significantly decreased expression in the BCL samples compared with controls (Table 2 and Figure 1B). All had a median fold-difference > ±2. No miRNAs had significantly different expression between TCL and controls. Two miRNAs had increased expression and one had decreased expression in TCL compared with BCL cases (Table 2 and Figure 2). The miR-130a-3p and miR-155-5p had a median fold-difference > ±2.

In the diagnostic pruned decision tree model classifying all lymphoma samples from control samples, miR-125a and miR-574a were selected (Figure 3A). The accuracy of the model was 86.79% (95% confidence interval [CI]: 0.78, 0.96) and all lymphoma samples were classified as such (recall = 1). Seven of 13 control samples were misclassified (recall = 0.46). To refine this model, BCL and TCL cases were separated along with controls (Figure 3B). In this model, miR-155-5p, miR-1 and miR-181b

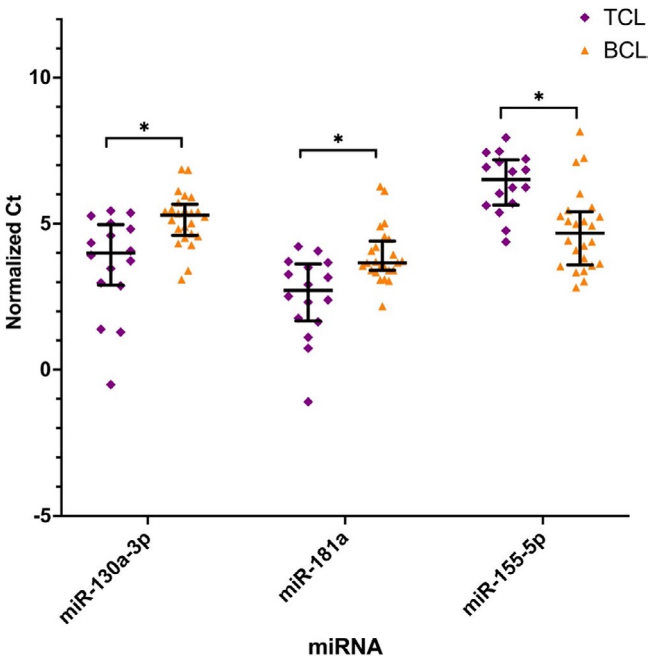

FIGURE 2 | The miRNAs significantly (p value < 0.05) differentially expressed between B-cell lymphoma (BCL) and T-cell lymphoma (TCL) groups. Values are shown as normalised cycle threshold (*Ct*) values. *p value < 0.05, **p value < 0.01, ***p value < 0.001. Benjamini–Hochberg corrected p values. Bar represents median with interquartile range.

were selected and resulted in an accuracy of 83.02% (95% CI: 0.73, 0.93). All control samples were appropriately classified (recall = 1). Five BCL cases were misclassified (four as TCL and one as control; recall = 0.79). Four TCL samples were misclassified (three as BCL and one as control; recall = 0.75). The area under the curve (AUC) ranged from 0.781 to 0.812 depending on the group comparison.

Fifteen single miRNAs were able to predict OS in the BCL group (Supporting Information Materials S9). Low expression represented a better probability of survival in 13/15 miRNAs. Ten miRNAs were able to predict OS in the TCL group (Supporting Information Materials S10). Low expression of miR-155-5p represented a better probability of survival in both lymphoma groups (Supporting Information Materials S9C and S10J) independently but not when the groups were combined. The miR-450a was similarly predictive in both groups independently, but low expression in the BCL (Supporting Information Materials S9I) group represented a better probability of survival, whereas it was high expression in the TCL group (Supporting Information Materials S10A). In the combined lymphoma group, 16 miRNAs were predictive of OS (Supporting Information Materials S11). The miR-194-5p and miR-199 were only predictive in the combined lymphoma group.

In the prognostic pruned decision tree model for OS in BCL (Figure 4), miR-125b-5p, miR-350 and let-7b-5p were selected. The miR-125b^{low}/miR-350^{high} group provided a protective hazard ratio (HR = 0.44; mean deviance [MD] = 0.33). This group had a significantly different OS compared with all other groups (MST = 650 days; range: 395–1289 days). Patients in the miR-125b^{high}/let-7b^{low} and miR-125b^{low}/miR-350^{low} groups had a slightly increased risk (HR = 1.2; MD = 0.05 and HR = 1.3; MD = 0.60, respectively) that were not significantly different from each other. These groups had an MST of 411 days (range: 356–460 days) and 265 days (range: 253–370 days), respectively. Finally, the miR-125b^{high}/let-7b^{high} group had an increased risk of death (HR = 3.5; MD = 0.56), the shortest OS (MST = 166 days; range: 67–244 days) and this group was significantly different from all others.

4 | Discussion

Multiple miRNA pruned decision tree models were able to accurately classify serum samples from patients with lymphoma versus controls. Regardless of subtype, the all-lymphoma model was able to classify all cases of lymphoma but had a high number of false positives (7 of 13 control samples; recall = 0.46). This resulted in an overall accuracy of 86.79% (95% CI: 0.78, 0.96). A higher rate of false positives may be acceptable if used as a screening test, since secondary imaging or further clinical examination could be pursued. The diagnostic model which accounted for lymphoma subtype had a lower accuracy (83.02% [95% CI: 0.73, 0.93]) but all controls were appropriately classified. Even though some BCL (four cases) and TCL (three cases) cases were inappropriately subtyped, only one case each was classified as controls (false negatives). Further refinement of these models may be required including the determination of acceptable false positive and false negative rates for future clinical implementation.

The results of this study support the importance of separating subtypes of lymphoma rather than combining them into one lymphoma group. All previous studies on miRNA profiles in canine lymphoma have found differences between B-cell and T-cell subtypes [4, 17, 18]. MiR-130a-3p and miR-155-5p had a significant median fold-difference > ±2 in TCL compared with BCL cases in this study. This is not surprising considering the vast differences in development and function of their non-neoplastic counterparts. The miRNAs, either from lymph node aspirates or in circulation, may serve as a novel way to phenotype lymphoma cases.

In the BCL group, miR-155-5p had the greatest statistically significant median fold-difference (4.34). It was also the first decision tree step that classified 19 of the 24 BCL samples. Tissue expression of miR-155-5p is controversial, as evidence supports its increased expression in human DLBCL, as part of the oncomiR miR-17-92 cluster, but it had decreased expression in canine DLBCL [14, 15]. This miRNA was not differentially expressed in serum or plasma in other dog studies [4, 16]. These results support the increased expression of this miRNA in BCL, similar to results from a systematic review of the human literature [34]. Differences in methodology and sample type may account for this variation between studies.

The miR-181a and miR-181c have increased expression in lymph node aspirates from dogs with TCL compared with healthy control dogs [4, 17, 18]. Although miR-181a and miR-181b did not maintain statistical significance with the Benjamini–Hochberg procedure between TCL cases and

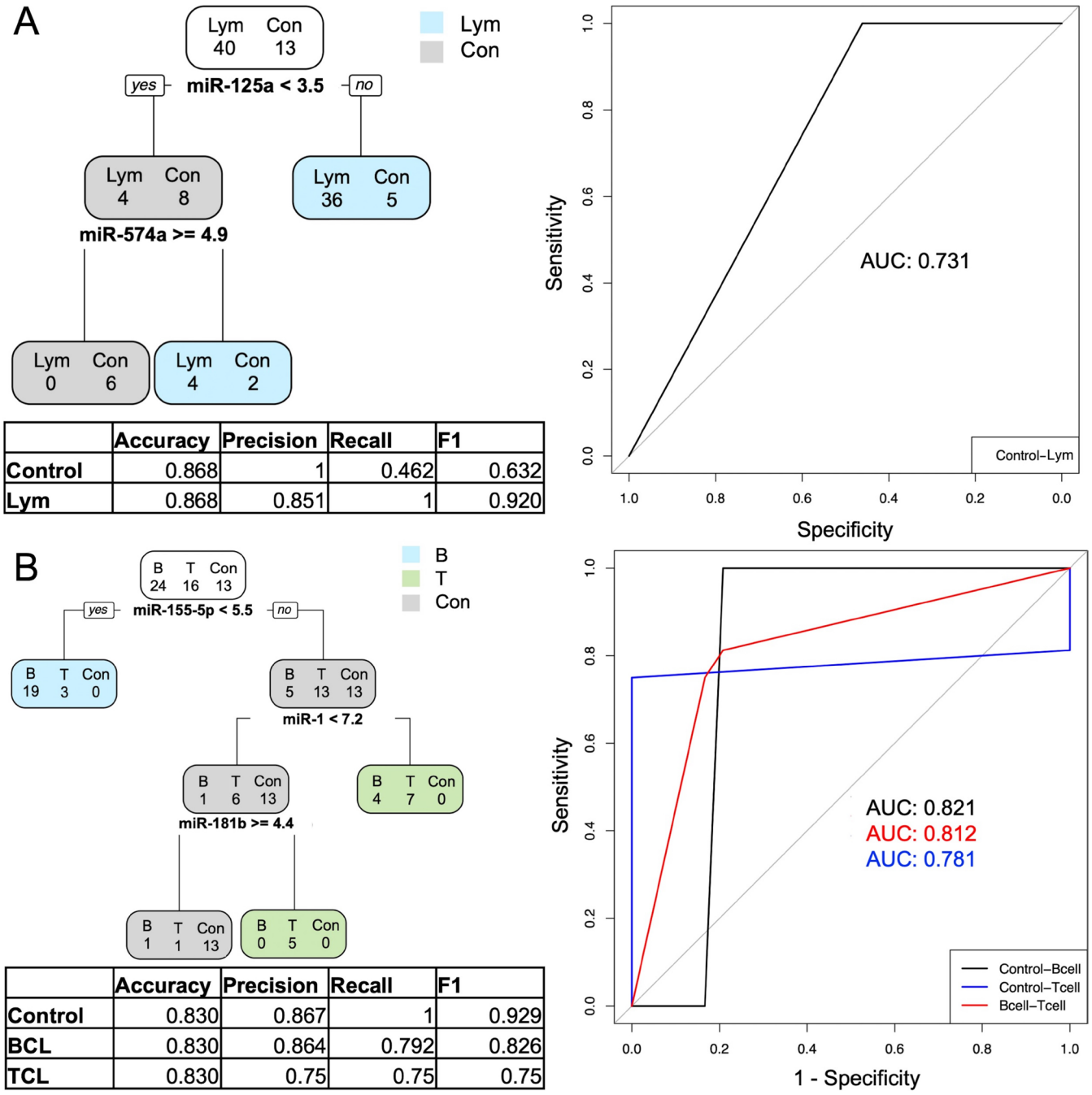

	Accuracy	Precision	Recall	F1
Control	0.868	1	0.462	0.632
Lym	0.868	0.851	1	0.920

	Accuracy	Precision	Recall	F1
Control	0.830	0.867	1	0.929
BCL	0.830	0.864	0.792	0.826
TCL	0.830	0.75	0.75	0.75

FIGURE 3 | Diagnostic pruned decision tree models classifying serum samples based on miRNA expression. Pruned decision tree model where each step is a cut-off based on normalised *Ct* value and a "yes" determination is always to the left. The table represents associated metrics (accuracy, precision, recall and F1) for each group and adjacent receiver operating characteristic curves with area under the curve (AUC) reported. (A) Model classifies known lymphoma (Lym) and control (Con) cases as lymphoma (blue boxes) or control (grey boxes) using miR-125a and miR-574a. (B) Model classifies known B-cell lymphoma (B; BCL), T-cell lymphoma (T; TCL) or control (Con) cases as B-cell lymphoma (blue boxes), T-cell lymphoma (green box) or control (grey boxes) using miR-155-5p, miR-1 and miR-181b.

controls, miR-181a had increased expression in TCL compared with BCL cases. The miR-181b also helped classify T-cell cases in the decision tree. The miR-181 family represents six different miRNAs in the vertebrate genome, which are highly conserved and linked by their shared seed region [35]. This family is important in T-cell and other haematopoietic cell differentiation [35]. In this study and other canine studies, each mature miR-181 investigated had importance in TCL classification [4, 17, 18].

Multiple miRNAs were associated with OS, including 15 miRNAs in the BCL group and 10 in the TCL group. Craig et al. (2019) reported high plasma expression of miR-155-5p in cases with shorter progression-free survival, and the current study found the same association with OS [4]. In Craig et al. (2019), patients with low expression of miR-150-5p in lymph node aspirates had decreased progression-free survival and OS in BCL [4]. The current study found the opposite; cases with high expression of miR-150-5p in serum had decreased OS. Fujiwara-Igarashi et al.

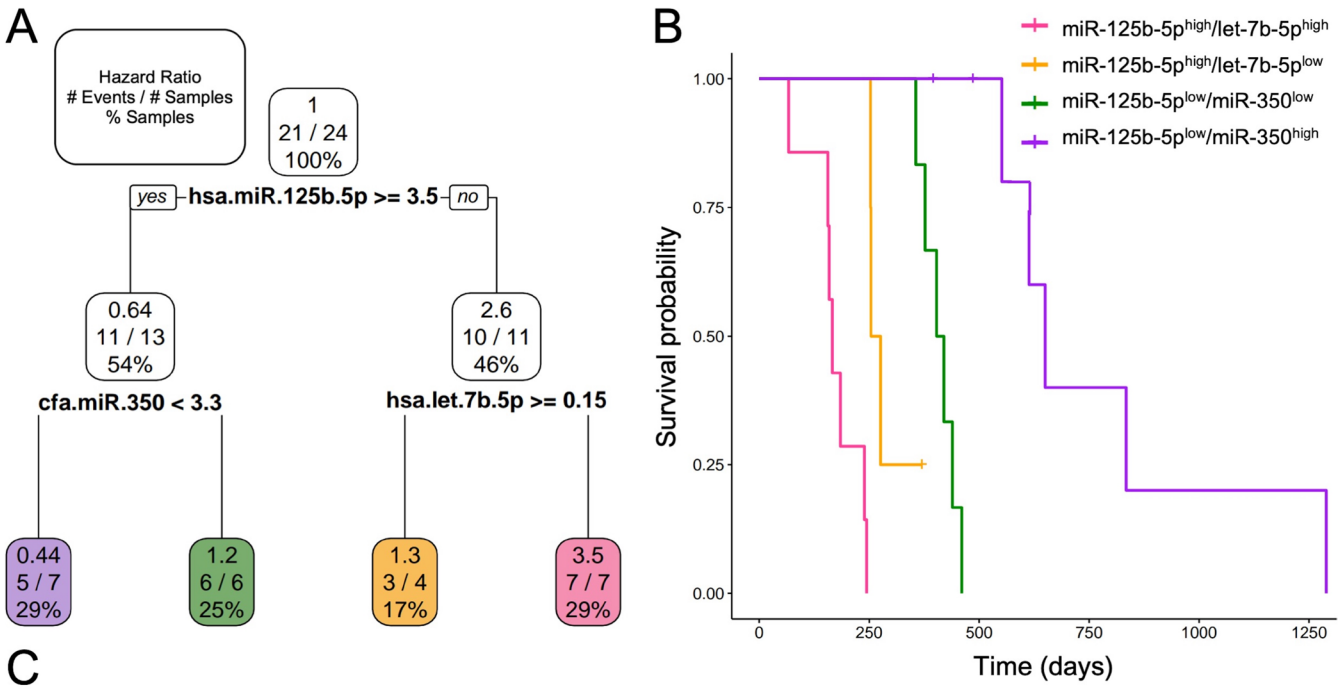

C

	MST (days); range (days)	miR-125b-5p^{high}/ let-7b-5p^{low} comparison	miR-125b-5p^{low}/ miR-350^{low} comparison	miR-125b-5p^{low}/ miR-350^{high} comparison
miR-125b-5p^{high}/ let-7b-5p^{high}	166; 67-244	p-value = 1.8E-02	p-value = 2.3E-03	p-value = 8.4E-04
miR-125b-5p^{high}/ let-7b-5p^{low}	265; 253-370	-	p-value = 2.0E-01	p-value = 4.2E-02
miR-125b-5p^{low}/ miR-350^{low}	411; 356-460	-	-	p-value = 2.3E-03
miR-125b-5p^{low}/ miR-350^{high}	650; 395-1289	-	-	-

FIGURE 4 | Multiple miRNA model using miR-125b-5p, miR-350 and let-7b-5p to predict overall survival in B-cell lymphoma patients receiving standard CHOP chemotherapy. (A) Pruned decision tree for overall survival classified samples into four groups with different hazard ratios (HRs). Each step (normalised *Ct* values used as cut-off) including the corresponding HR, number of events defined by death due to progressive B-cell lymphoma out of the total number of samples, and percentage samples in each group. (B) Kaplan–Meier survival curve for each of the groups. (C) Median survival time (days) with range (days) for each group and the group comparison corresponding *p* values (with Bonferroni correction).

(2015) used serum samples and demonstrated a link between let-7b and miR-25 and grade (high vs. low) [16]. The results in the current study found let-7b-5p was only correlated with OS in BCL cases. The let-7b-5p was also included in the prognostic multiple miRNA decision tree model. The differences between previous studies and the current study could reflect differences in technology used, differences in miRNA expression between serum and plasma samples and/or differences in case classification [4, 16, 36].

The multiple miRNA pruned decision tree model for OS in BCL cases better refined the survival groups compared with single miRNAs. For example, miR-125b-5p alone was predictive of OS with 13 patients in the low expression/long survival group (MST = 460 days) and 11 patients in the high expression/short survival group (MST = 239 days). This miRNA was the first step in our multiple miRNA model. With the addition of let-7b-5p and miR-350, which alone were also both predictive of OS, four groups were created. The longest surviving group consisted of 7 dogs and had a MST of 650 days. The shortest surviving group consisted of 7 dogs and had a MST of 166 days. These are different from the predictive ability of miR-125b-5p alone and help to determine cases with very short and very long survival from those with the more typical range of 300–360 days, as demonstrated by the intermediate groups consisting of 10 dogs total (range: 253–460 days).

Hemolysis is a challenge when measuring miRNAs in plasma or serum as erythrocytes contain miRNAs and alter results proportional to the degree of hemolysis [22, 32]. Visual inspection is insensitive in determining the degree of hemolysis, and more sensitive methods such as spectrophotometry should be used [23, 37]. Certain miRNAs are known to have relative abundance in erythrocytes, such as miR-451a, miR-92-3p and miR-16; however, many others are unknown [32, 33]. Thus far, there is no consensus method described on how to account for or adjust for hemolysis when evaluating miRNAs. Therefore, miRNAs were investigated to determine which may be associated with hemolysis and should be interpreted with caution as previously described [21, 25]. None of our miRNAs differentially expressed or found to have prognostic value in this study had R^2 values

above these three reference miRNAs. Evidence suggests that miR-21-5p is not altered with hemolysis, so those with R^2 values less than that of miR-21-5p were deemed to be unlikely to be from hemolysis [22, 32]. None of the miRNAs selected in the diagnostic or prognostic analyses were strongly associated with hemolysis. Amongst those between the reference miRNAs, most determined to be important in this study trended away from an association with hemolysis.

A limitation of RT-qPCR is the pre-determination of which miRNAs will be investigated, which narrows the scope of the study. The pooled samples and use of the miScript Canine miRNome arrays assisted in determining which miRNAs to assay but do not include all possible miRNAs. The population investigated and thus the results only apply to patients receiving treatment for lymphoma. The treatment protocols and their success were variable in the TCL group, and this precluded the evaluation of multiple miRNA prognostic models for TCL patients. Studies including a larger number of prospective samples with standardised treatment and specific subtypes within BCL and TCL would be helpful in validating these results.

The miRNAs are a potential tool for diagnosis and prognosis of canine lymphoma. We found multiple differentially expressed miRNAs in serum in cases of BCL compared with controls and TCL. Multiple miRNA models were better able to refine the classification of disease and diagnosis compared with single miRNAs, including predicting outcome in BCL cases.

Acknowledgements

The authors thank the staff of the Ontario Veterinary College's Veterinary Biobank for providing samples and clinical information, and Dr. Karlee Craig for her collection of clinical information. We also thank the owners and veterinarians for patient samples and providing care to the patients involved in this study. Funding provided to Geoffrey A. Wood from NSERC (401622) and OVC Pet Trust (55680) and to Latasha Ludwig from NSERC Vanier Canadian Graduate Scholarship and OVC Fellowship.

Conflicts of Interest

The authors declare no conflicts of interest.

Cell Line Authentication Statement

No cell lines were used in this research.

Data Availability Statement

The data that support the findings of this study are available from the corresponding author upon reasonable request.

References

1. D. Vail, M. Pinkerton, and K. Young, "Hematopoietic Tumors," in *Withrow and MacEwen's Small Animal Clinical Oncology*, 6th ed., ed. D. Vail, D. Thamm, and J. Liptak (Elsevier, 2020), 688–772.

2. V. E. Valli, M. S. Myint, A. Barthel, et al., "Classification of Canine Malignant Lymphomas According to the World Health Organization Criteria," *Veterinary Pathology* 48, no. 1 (2011): 198–211.

3. V. Valli, D. Bienzle, D. Meuten, and K. Linden, "Tumors of the Hemolymphatic System," in *Tumors in Domestic Animals*, 5th ed., ed. D. J. Meuten and T. L. K. Meuten (John Wiley & Sons Inc., 2017), 203–321.

4. K. K. L. Craig, G. A. Wood, S. M. Keller, A. J. Mutsaers, and R. D. Wood, "MicroRNA Profiling in Canine Multicentric Lymphoma," *PLoS One* 14, no. 12 (2019): e0226357.

5. L. Thalheim, L. E. Williams, L. B. Borst, J. E. Fogle, and S. E. Suter, "Lymphoma Immunophenotype of Dogs Determined by Immunohistochemistry, Flow Cytometry, and Polymerase Chain Reaction for Antigen Receptor Rearrangements," *Journal of Veterinary Internal Medicine* 27, no. 6 (2013): 1509–1516.

6. N. Deravi, O. Berke, J. P. Woods, and D. Bienzle, "Specific Immunotypes of Canine T Cell Lymphoma Are Associated With Different Outcomes," *Veterinary Immunology and Immunopathology* 191 (2017): 5–13.

7. A. Wolf-Ringwall, L. Lopez, R. Elmslie, et al., "Prospective Evaluation of Flow Cytometric Characteristics, Histopathologic Diagnosis and Clinical Outcome in Dogs With Naïve B-Cell Lymphoma Treated With a 19-Week CHOP Protocol," *Veterinary and Comparative Oncology* 18, no. 3 (2020): 342–352.

8. J. Matsuzaki and T. Ochiya, "Circulating MicroRNAs and Extracellular Vesicles as Potential Cancer Biomarkers: A Systematic Review," *International Journal of Clinical Oncology* 22, no. 3 (2017): 413–420.

9. P. S. Mitchell, R. K. Parkin, E. M. Kroh, et al., "Circulating MicroRNAs as Stable Blood-Based Markers for Cancer Detection," *Proceedings of the National Academy of Sciences of the United States of America* 105, no. 30 (2008): 10513–10518.

10. F. Balzano, M. Deiana, S. Dei Giudici, et al., "MiRNA Stability in Frozen Plasma Samples," *Molecules* 20, no. 10 (2015): 19030–19040.

11. C. Glinge, S. Clauss, K. Boddum, et al., "Stability of Circulating Blood-Based MicroRNAs – Pre-Analytic Methodological Considerations," *PLoS One* 12, no. 2 (2017): e0167969.

12. Z. Li, D. Chen, Q. Wang, et al., "mRNA and MicroRNA Stability Validation of Blood Samples Under Different Environmental Conditions," *Forensic Science International: Genetics* 55 (2021): 102567.

13. H. Asada, H. Tomiyasu, T. Uchikai, et al., "Comprehensive Analysis of miRNA and Protein Profiles Within Exosomes Derived From Canine Lymphoid Tumour Cell Lines," *PLoS One* 14, no. 4 (2019): e0208567.

14. N. O. Elshafie, M. Gribskov, N. I. Lichti, E. Sayedahmed Ekramy, M. O. Childress, and A. P. Dos Santos, "miRNome Expression Analysis in Canine Diffuse Large B-Cell Lymphoma," *Frontiers in Oncology* 13 (2023): 1238613.

15. N. O. Elshafie, N. C. D. Nascimento, N. I. Lichti, A. L. Kasinski, M. O. Childress, and A. P. D. Santos, "MicroRNA Biomarkers in Canine Diffuse Large B-Cell Lymphoma," *Veterinary Pathology* 58, no. 1 (2021): 34–41, https://doi.org/10.1177/0300985820967902.

16. A. Fujiwara-Igarashi, H. Igarashi, N. Mizutani, et al., "Expression Profile of Circulating Serum MicroRNAs in Dogs With Lymphoma," *Veterinary Journal* 205, no. 2 (2015): 317–321.

17. M. Mortarino, G. Gioia, M. E. Gelain, et al., "Identification of Suitable Endogenous Controls and Differentially Expressed MicroRNAs in Canine Fresh-Frozen and FFPE Lymphoma Samples," *Leukemia Research* 34, no. 8 (2010): 1070–1077.

18. E. Uhl, P. Krimer, P. Schliekelman, S. M. Tompkins, and S. Suter, "Identification of Altered MicroRNA Expression in Canine Lymphoid Cell Lines and Cases of B- and T-Cell Lymphomas," *Genes, Chromosomes & Cancer* 50, no. 11 (2011): 950–967.

19. C. Zhang, C. Sun, Y. Zhao, et al., "Overview of MicroRNAs as Diagnostic and Prognostic Biomarkers for High-Incidence Cancers in 2021," *International Journal of Molecular Sciences* 23, no. 19 (2022): 11389, https://doi.org/10.3390/ijms231911389.

20. A. Beheshti, K. Stevenson, C. Vanderburg, et al., "Identification of Circulating Serum Multi-MicroRNA Signatures in Human DLBCL Models," *Scientific Reports* 9, no. 1 (2019): 17161.

21. L. Ludwig, M. Edson, H. Treleaven, et al., "Plasma MicroRNA Signatures Predict Prognosis in Canine Osteosarcoma Patients," *PLoS One* 19, no. 12 (2024): e0311104, https://doi.org/10.1371/journal.pone.0311104.

22. M. B. Kirschner, J. J. B. Edelman, S. C. H. Kao, M. P. Vallely, N. Van Zandwijk, and G. Reid, "The Impact of Hemolysis on Cell-Free MicroRNA Biomarkers," *Frontiers in Genetics* 24, no. 4 (2013): 94.

23. M. B. Kirschner, S. C. Kao, J. J. Edelman, et al., "Haemolysis During Sample Preparation Alters MicroRNA Content of Plasma," *PLoS One* 6, no. 9 (2011): e24145.

24. O. Fortunato, M. Boeri, C. Verri, et al., "Assessment of Circulating MicroRNAs in Plasma of Lung Cancer Patients," *Molecules* 19, no. 3 (2014): 3038–3054.

25. L. Ludwig, H. Treleaven, A. Khachadoorian, et al., "MicroRNAs in Serum and Tissue Can Differentiate Splenic Hemangiosarcoma From Other Splenic Masses in Dogs," *Veterinary Pathology* (2025), https://doi.org/10.1177/03009858251317466.

26. R Core Team, *R: A Language and Environment for Statistical Computing* (R Core Team, 2021), http://www.R-project.org/.

27. C. L. Andersen, J. L. Jensen, and T. F. Ørntoft, "Normalization of Real-Time Quantitative Reverse Transcription-PCR Data: A Model-Based Variance Estimation Approach to Identify Genes Suited for Normalization, Applied to Bladder and Colon Cancer Data Sets," *Cancer Research* 64, no. 15 (2004): 5245–5250.

28. J. Vandesompele, K. De Preter, F. Pattyn, et al., "Accurate Normalization of Real-Time Quantitative RT-PCR Data by Geometric Averaging of Multiple Internal Control Genes," *Genome Biology* 3, no. 7 (2002): research0034.1.

29. T. D. Schmittgen and K. J. Livak, "Analyzing Real-Time PCR Data by the Comparative CT Method," *Nature Protocols* 3, no. 6 (2008): 1101–1108.

30. Y. Benjamini and Y. Hochberg, "Controlling the False Discovery Rate: A Practical and Powerful Approach to Multiple Testing," *Journal of the Royal Statistical Society, Series B (Statistical Methodology)* 57, no. 1 (1995): 289–300.

31. A. Kassambara, M. Kosinski, and P. Biecek, *survminer: Drawing Survival Curves Using 'ggplot2'* (GitHub, 2021).

32. M. Aguilera-Rojas, S. Sharbati, T. Stein, M. Candela Andrade, B. Kohn, and R. Einspanier, "Systematic Analysis of Different Degrees of Haemolysis on miRNA Levels in Serum and Serum-Derived Extracellular Vesicles From Dogs," *BMC Veterinary Research* 18, no. 1 (2022): 355.

33. C. C. Pritchard, E. Kroh, B. Wood, et al., "Blood Cell Origin of Circulating MicroRNAs: A Cautionary Note for Cancer Biomarker Studies," *Cancer Prevention Research* 5, no. 3 (2012): 492–497.

34. H. Due, P. Svendsen, J. S. Bødker, et al., "miR-155 as a Biomarker in B-Cell Malignancies," *BioMed Research International* 2016 (2016): 1–14.

35. A. Bell-Hensley, S. Das, and A. McAlinden, "The miR-181 Family: Wide-Ranging Pathophysiological Effects on Cell Fate and Function," *Journal of Cellular Physiology* 238, no. 4 (2023): 698–713.

36. K. Wang, Y. Yuan, J. H. Cho, S. McClarty, D. Baxter, and D. J. Galas, "Comparing the microRNA Spectrum Between Serum and Plasma," *PLoS One* 7, no. 7 (2012): e41561, https://doi.org/10.1371/journal.pone.0041561.

37. P. Tiberio, M. Callari, V. Angeloni, M. G. Daidone, and V. Appierto, "Challenges in Using Circulating miRNAs as Cancer Biomarkers," *BioMed Research International* 2015 (2015): 1–10.

Supporting Information

Additional supporting information can be found online in the Supporting Information section.